FULL PAPER

Labeling and Tracking P2 Purinergic Receptors in Living Cells Using ATP-Conjugated Quantum Dots

Shan Jiang, Aiping Liu, Hongwei Duan, Jianchow Soo, and Peng Chen**

It has been increasingly recognized that adenosine-5′-triphosphate (ATP) signaling through P2 purinergic receptors has a diverse influence on cell functions and human health. In this contribution, a simple and non-invasive method to specifically label P2 receptors using ATP-conjugated quantum dots (QDs) is demonstrated. In addition, the endocytosis, vesicular trafficking, and recycling of QD-labeled P2 receptors are studied under different physiological conditions using confocal and total internal reflection fluorescence microscopy.

1. Introduction

Adenosine-5′-triphosphate (ATP), famous as the universal fuel inside cells, is also a critical signaling molecule mediating a spectrum of cellular functions, such as neurotransmission, hormone secretion, proliferation, differentiation, and apoptosis.[1] ATP signaling acts through two types of membrane-bound purinergic receptors, P2X ionotropic receptors which are ligand-gated ion channels and P2Y metabotropic receptors which are G protein-coupled receptors.[2]

Despite their increasingly recognized importance in cell biology and as drug targets (for cardiovascular diseases, pain, inflammation, cystic fibrosis, etc.),[3] the physiology of ATP (P2 purinergic) receptors is far from been fully understood. Imaging the distribution and the "life" of ATP receptors in live cells would obviously be instrumental in elucidating their functions. In view of this, overexpression of P2X receptors tagged with green fluorescent protein (GFP) has been utilized to reveal the distribution, density, ligand-activated clustering, and internalization of the receptor.[4] However, such a molecular biology approach is non-trivial, involving plasmid construction and transfection. The expression of such protein chimera is often of low efficiency. In addition, GFP, just like other organic fluorophores, does not allow long-term imaging due to photobleaching.

In contrast to the conventional fluorescent dyes and proteins, quantum dots (QDs) exhibit superior optical properties including high and uniform brilliance, broad absorption spectra, narrow and size-tunable emission, and excellent photostability. They have been successfully utilized to label various molecular targets in a number of cell types, providing unique insights into the distribution, transport, and functions of these molecules.[5] Herein, we specifically and readily labeled ATP receptors on live neuroendocrine PC12 cells using ATP-conjugated quantum dots (QD-ATP). Additionally, the endocytosis, vesicular trafficking, and recycling of these receptors was investigated using confocal and total internal reflection fluorescence microscopy (TIRFM). Furthermore, we demonstrate that the vesicular trafficking and recycling of ATP receptors were enhanced by nerve growth factor (NGF) and starvation, implying the involvement of these receptors in the neuronal differentiation and apoptosis.

S. Jiang, A. Liu, Prof. H. Duan, J. Soo, Prof. P. Chen
Division of Bioengineering
School of Chemical & Biomedical Engineering
Nanyang Technological University
70 Nanyang Drive, Singapore 637457
E-mail: hduan@ntu.edu.sg; chenpeng@ntu.edu.sg

DOI: 10.1002/adfm.201100472

2. Results and Discussion

2.1. Synthesis of QD-ATP

Figure 1 illustrates the scheme for functionalization of ATP molecules onto QD. Core-shell QDs (CdSe/CdS/ZnS) were synthesized and coated with the amphiphilic copolymer of maleic anhydride and octadecene (PMO) as previously described,[6] resulting in highly stable QDs with carboxylic acid functionalities. The coated QDs (QD-PMO) were further modified to link phenylboronic acid (PBA) tags on their surfaces. Subsequently, 4-[(2-aminoethyl)carbamoyl]phenylboronic acid (AECPBA), which can stably bind with the 1,2 diols in the ATP structure,[7] was conjugated with the carboxylic acid groups on QD-PMO in the presence of EDAC in pH 7.4 borate buffer. The diameter of the coated QDs is about 12–14 nm.[8] After removing free QD-PMO and AECPBA by ultrafiltration, the resulting QD-AECPBA complexes were allowed to react with ATP (1 mg mL^{-1}) in a 0.2 M borate buffer solution (pH 7.4) for 4 h at room temperature, followed by ultrafiltration (5000 rpm for 8 min) with DI water for 2 times to remove excess ATP molecules. UV–vis, fluorescence spectroscopy, and gel electrophoresis of QD-PMO, QD-AECPBA, and QD-ATP are provided in the Supporting Information, indicating the effects of each functionalization step. The quantum yield of the QDs dropped by 25%, probably due to the presence of the adenosine group in ATP. QD-AECPBA showed slower gel mobility than that of QD-PMO due to the reduced surface charge density after replacing carboxylic acid groups (pKa~5–6) into PBA (pKa~7.8) groups. Conjugation of ATP to QD-AECPBA increased the

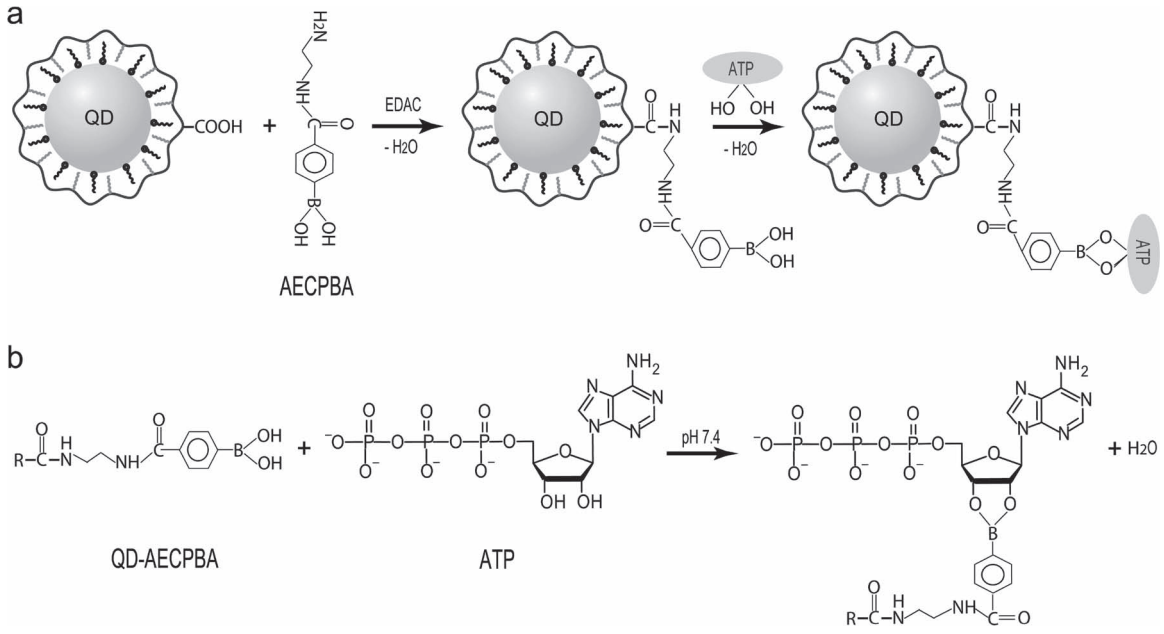

Figure 1. a) Schematic illustration of the synthesis of QD-ATP. b) Covalent reaction between AECPBA and ATP.

gel mobility, resulting from the increased surface charge density because of the three phosphate groups in ATP molecules. Freshly prepared QD-ATP was used for all experiments to minimize the hydrolysis or detaching of ATP molecules.

2.2. QD-ATP Can Trigger Ca^{2+} Signaling

ATP is known to trigger rapid increase of intracellular Ca^{2+} concentration ($[Ca^{2+}]_i$) by inducing Ca^{2+} influx through P2X channels and release of Ca^{2+} from the endoplasmic reticulum.[9] To test the functionality of QD-ATP, we applied it (140 nM) to PC12 cells which abundantly express P2 purinergic receptors, while $[Ca^{2+}]_i$ was continuously monitored by single-cell photometry. As shown in **Figure 2**, QD-ATP triggered acute increase of $[Ca^{2+}]_i$. In contrast, the filtrate (5000 rpm for 8 min) of the Ca^{2+} evoking QD-ATP solution did not produce any Ca^{2+} signal, indicating that the observed Ca^{2+} signal is indeed due to the presence of QD-ATP instead of the free residual ATP molecules resulted from incomplete filtration during synthesis or detaching of ATP molecules from QDs. Furthermore, QD-AECPBA (the immediate precursor of QD-ATP) did not elicit significant signal. These observations suggest that ATP preserves its functionality after conjugation and QD-ATP can specifically bind and acutely activate P2 receptors.

2.3. Cellular Internalization of QD-ATP

Confocal fluorescence microscopy was then used to visualize the labeling of P2 receptors with QD-ATP. After PC12 cells were exposed to QD-ATP (20 nM) for 15 min followed by washing, staining of QD-ATP on the cell surface was observed (**Figure 3**a). The observed fluorescent puncta of QD-ATP on the cell membrane suggests that P2 receptors aggregate in the hot spots (microdomains), agreeing with the previous reports.[4] The aggregation of P2 receptors may be partly due to oligomerization of the receptors.[10] In the control experiments, when overwhelming free ATP (3 mM) was added together, QD-ATP staining was completely eliminated (Figure S3). This again unambiguously demonstrates the specific recognition between QD-ATP and the P2 receptors. As shown in Figure 3a–d, QD-ATPs remained mostly on the cell surface during the initial 20 min after pre-incubation, then, were mostly internalized (endocytosed) within 1 h. The internalized QD-ATPs segregated into vesicles instead of individually dispersing in the cytosol. It has been reported that ATP activation triggers endocytosis of P2 receptors within 30 s in ganglion neurons.[4a,11] However,

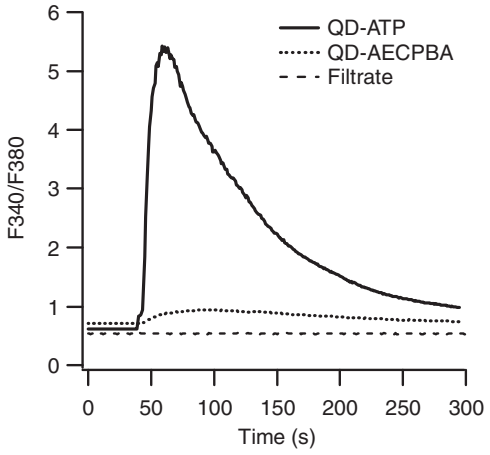

Figure 2. Ratiometric fluorescence measurement of intracellular increase of Ca^{2+} concentration stimulated by locally delivered 140 nM QD-ATP containing bath solution or its filtrate or 140 nM QD-AECPBA containing solution, using an application glass pipette positioned near the target cell.

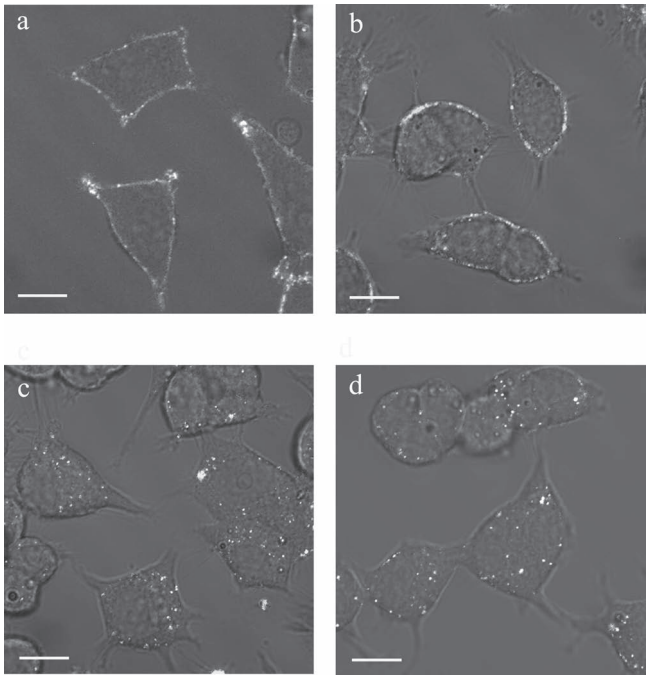

Figure 3. Staining and internalization of QD-ATP in PC12 cells. Superimposition of the fluorescence image and bright-field image of PC12 cells taken at a) 0 min, b) 20 min, c) 40 min, d) 60 min after the cells were exposed to 20 nM QD-ATP for 15 min. Scale bar = 10 μm.

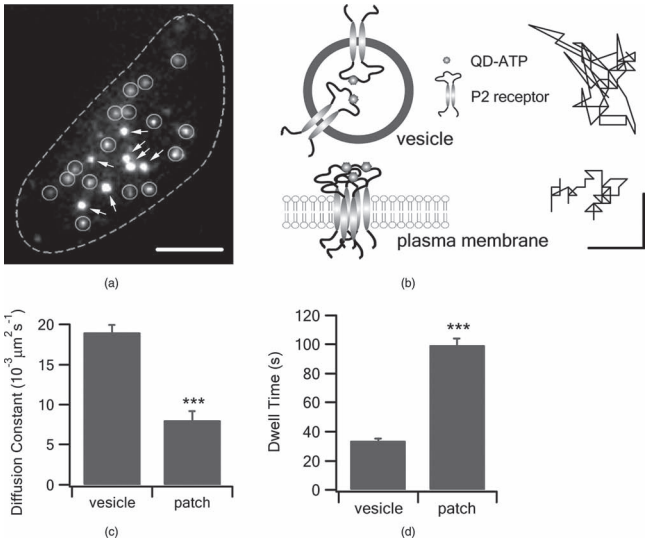

Figure 4. a) Typical TIRFM image of a PC12 cell showing the QD-ATP vesicles (indicated by circles) in the subplasmalemmal region and the cell membrane patches with QD-ATP cluster (indicated by arrows). Scale bar = 5 μm. b) Illustration of QD-ATP vesicle (top) and QD-ATP membrane patches (bottom) and their typical trajectories of lateral movement. The vertical and horizontal scale bars = 0.5 μm. c,d) The statistics (12 cells) of the diffusion constant and dwell time of QD-ATP vesicles (n = 959) and QD-ATP membrane patches (n = 118). The error bars indicate the standard errors. Student's *t*-test: *** $p < 0.001$ versus vesicle.

our experiments suggest that such triggered rapid internalization is absent in PC12 cells, similar to the observations in hippocampal neurons.[4b]

2.4. Trafficking of QD-ATP Invesitaged by TIRFM

Furthermore, we investigated the vesicle trafficking and recycling of P2 receptors using total internal reflection fluorescence microscopy (TIRFM), which evanescently illuminates the thin subplasmalemmal region (<200 nm thick) just above the interface between the glass coverslip and the cell membrane. Since the evanescence field decays exponentially with the distance away from the interface, TIRFM is powerful in revealing the molecular events (e.g., vesicle trafficking and fusion) occurring at or immediately adjacent to the cell membrane with minimal interference from the background and with a higher temporal resolution than confocal microscopy.[12]

After preincubating PC12 cells with 1 nM of QD-ATP for 1 h, time-lapse images were taken under TIRFM for 2 min with a sampling frequency of 2 Hz. Individual QD-ATP vesicles (vesicles endocytosed with QD-ATP/P2 receptor complex) in the subplasmalemmal region can be clearly resolved (bright dots highlighted by circles in **Figure 4**a; and illustration in Figure 4b top). Similar to secretory vesicles in neurons and neuroendorince cells, QD-ATP vesicles undertake constant lateral movement (parallel to the cell membrane) and vertical movement (transition between the inner cytosol and the subplasmalemmal region as shown by appearance, disappearance, or fluctuation in vesicle fluorescence).[13] The trajectory of a vesicle's lateral movement is depicted in Figure 4b (top). The statistics of the lateral diffusion constant and dwell time of QD-ATP vesicles in the subplasmalemmal region are given in Figure 4c–d. It is noted that the diffusion of the QD-ATP vesicles is about ten times faster than the hormone-containing large dense core secretory vesicles in PC12 cells,[14] suggesting their distinct identities.

Different from the mobile intracellular vesicles, a few inactive and relatively large QD-ATP clusters can be identified (indicated by arrows in Figure 4a). They are especially bright and very stable in fluorescence intensity, implying that they are close to the glass coverslip and do not move in the vertical direction. They remain on the cell membrane for a relatively long time or throughout the entire imaging period (2 min) and drift laterally at a much slower rate as compared to the QD-ATP vesicles (Figure 4c-d). For further comparison, the mean square displacement (MSD) plots of a representative QD-ATP vesicle and a membrane patch is provided in Figure S4. Therefore, we conclude that these are membrane patches (microdomains) enriched with ATP receptors (as illustrated in Figure 4b bottom), instead of intracellular vesicles.

It has been revealed by TIRFM studies that both the lateral and vertical trafficking dynamics of secretory vesicles directly and positively relate to the vesicle fusion competence and the overall secretion kinetics.[12b,15] Therefore, it is conceivable that the trafficking of QD-ATP vesicles reflects the dynamic recycling (thus functioning) of P2 receptors. We have also observed disappearance of the stable membrane patches due to vesicular endocytosis (**Figure 5**a) and appearance (or arrival) of new stable membrane patches due to fusion of the QD-ATP vesicles with the plasma membrane (exocytosis) (Figure 5b). These events directly indicate the recycling dynamics of P2 receptors.

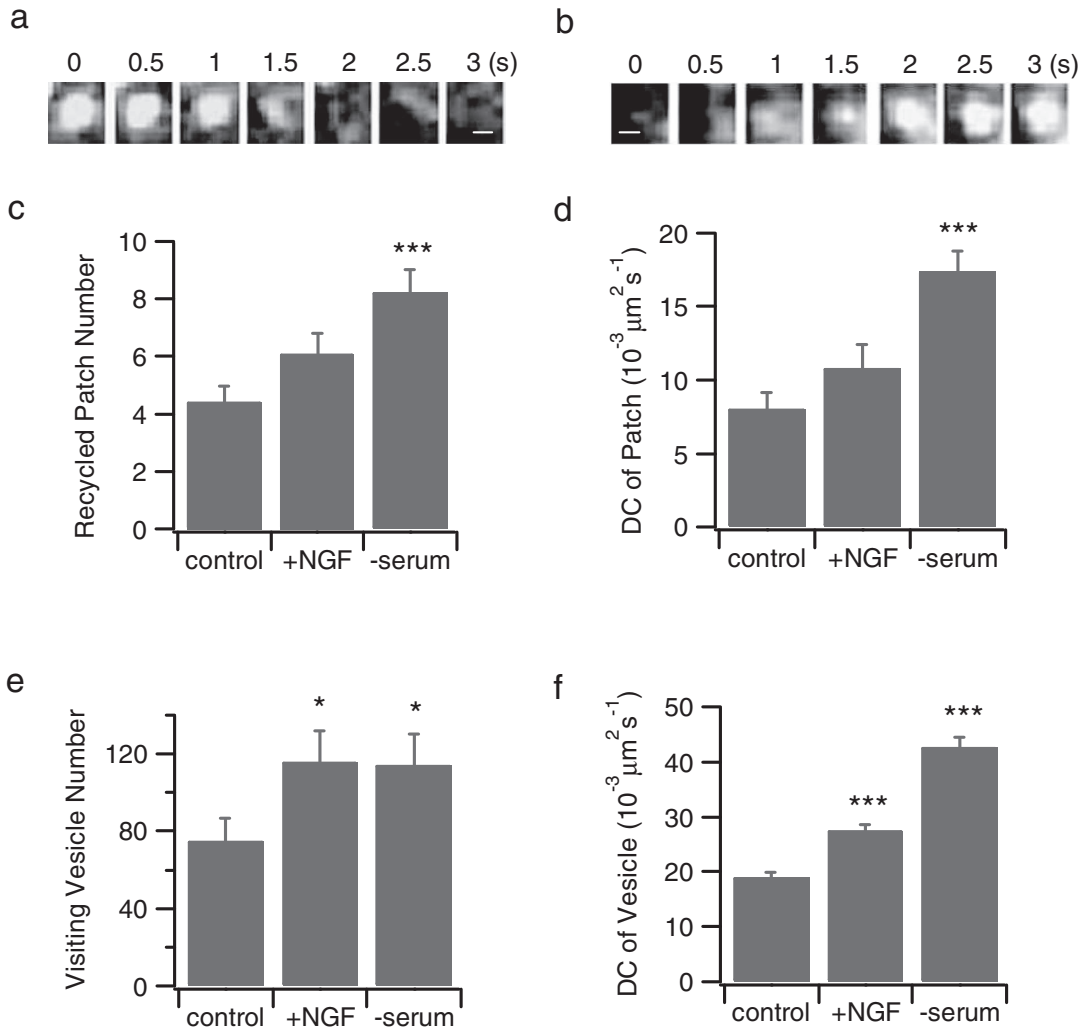

Figure 5. a) An endocytostic event of membrane patch enriched with QD-ATP/P2 receptor complex. b) Exocytotic event of a vesicle previously endocytosed with QD-ATP/P2 receptor complex. c) The total endocytosed and exocytosed (recycled) number of QD-ATP membrane patches. (d) The diffusion constant of QD-ATP membrane patches. e) The visiting number of QD-ATP vesicles. f) The diffusion constant of QD-ATP vesicles. Scale bars in (a) and (b) are 0.5 μm. The statistics is obtained from 959 vesicles and 118 patches in 12 untreated control cells, 1331 vesicles and 119 patches in 11 NGF treated cells, 1292 vesicles and 120 patches in 11 cells cultured in serum free medium. The error bars indicate the standard errors. Student's *t*-test: *** $p < 0.001$, * $p < 0.05$ versus control. DC = diffusion constant.

It has been shown that P2 receptor retains its function within the degradative environment of the lysosome by the virtue of its N-linked glycans, and they recycle to the plasma membrane in response to intense or continuous stimulation.[16] Also seen from Figure 5a and b, the size of the membrane patches (membrane domains enriched with P2 receptors) is about 1 μm, consistent with the previously reported.[4a] These microdomains mediate localized and synergistic reactions.

A QD can be functionalized with many ATP molecules. But the observed aggregation of ATP receptors (Figure 3a and 4a) is unlikely to be due to massive crosslinking induced by QD binding with multiple P2 receptors, because: i) The size of our QDs (12–14 nm) is similar to that of a single receptor molecule. And the effective contact area between such a small sphere with the flat cell membrane is even smaller; therefore, one QD may only bind with a few receptors. ii) The membrane domains (1 μm in size) lightened by the bound QDs could accommodate thousands of P2 receptors. iii) Our QDs do not crosslink with each other because QD aggregates were not observed in the gel electrophoresis experiments (Figure S2).

A number of studies have demonstrated that, through stimulating the MAPK/ERK pathway, activation of P2 purinergic receptors promotes survival and inhibits starvation-induced apoptosis,[17] and facilitates nerve growth factor (NGF)-induced neuronal differentiation and neurite growth of PC12 cells.[18] Using TIRFM, we examined the trafficking of QD-ATP vesicles and the recycling of QD-ATP membrane patches in presence of NGF stimulation (200 ng mL^{-1} for 4 h) or when the cells were cultured without serum for 6 h (starvation conditions that induce apoptosis). As shown by Figure 5c–d, under starvation, the total number of endocytosis and exocytosis of the QD-ATP membrane patches (recycled patches) and their lateral diffusion were significantly increased. In addition, both lateral vesicle trafficking (as indicated by the lateral diffusion constant) and vertical vesicle trafficking (as indicated by

the number of arriving vesicles which is roughly balanced by the number of retrieving vesicles) were enhanced by NGF and starvation (Figure 5e–f). These observations corroborate the links of the P2 receptor functions to the neuronal differentiation and apoptosis pathways. Confocal and TIRFM experiments were also conducted on neuronal differentiated PC12 cells. It was found that QD-ATP vesicles and membrane clusters were also active in the grown neurites. In some cells, they were enriched in the growth cone of the neurite, further implying the role of P2 receptors in neurite outgrowth (Figure S5).

3. Conclusions

In summary, we have demonstrated a simple approach to specifically label P2 purinergic receptors and monitor their trafficking and recycling using ATP-functionalized quantum dots. It is the first time dynamic data on P2 receptor trafficking with sub-second resolution has been provided, and related to neuronal differentiation and apoptosis. This study demonstrates the potentials of QDs in providing a novel tool to study the physiology of P2 receptors which underlies various critical diseases and cell functions.

4. Experimental Section

Cell culture, Treatment, and Bath Solution: PC12 cells (American Type Culture Collection) were cultured in Advanced RPMI medium 1640 (Gibco) supplemented with 5% (v/v) heat-inactivated horse serum (Gibco), 10% heat-inactivated fetal bovine serum (Gibco), and 1% penicillinstreptomycin (Gibco) at 37 °C in 5% CO_2/air. In some TIRFM experiments, cells were starved in serum-free Advanced RPMI medium for 6 h or incubated with NGF (200 ng ml^{-1}) for 4 h, followed by incubation with QD-ATP (1 nM) for 1 h prior to imaging. The bath solution used for imaging contained (titrated to pH 7.2) NaCl (150 mM), KCl (2.4 mM), $MgCl_2$ (2 mM), $CaCl_2$ (2 mM), glucose (10 mM), and HEPES (10 mM).

Ca^{2+} Imaging: PC12 cells were incubated with Fura2-AM (5 μM, a membrane permeable Ca^{2+} sensitive dye) for 45 min in a serum-free medium. Prior to recording in the bath solution, the cells were incubated in the fresh medium for >30 min to allow removal of the acetoxymethyl esters of Fura2-AM and consequently the retention of dye. PC12 cells were then stimulated by QD-ATP or QD-AECPBA (140 nM) while the intracellular Ca^{2+} was reported by the ratio of fluorescence emission (at 550 nm) subjecting to 340 and 380 nm excitation (F340/F380) using a single-cell photometry system (TILL Photonics, GmbH).[15b]

Confocal Imaging: Cells were incubated with QD-ATP (20 nM) for 15 min and then washed with bath solution for three times. To investigate time-dependent cellular uptake of QD-ATP, cells were imaged at progressive time points of 0, 20, 40, and 60 min after the pre-incubation of QD-ATP, using a confocal microscope (Zeiss LSM 510) with a 63× oil objective and a 488 nm excitation laser.

TIRFM Imaging: TIRFM was carried out using a Zeiss Axiovert 200 inverted microscope system (Carl Zeiss, Germany) equipped with a 100× oil-immersed objective (1.45 NA). QD was excited by a 458 nm laser, and the emission was collected at 620 nm. Time-lapse images were taken by an EMCCD camera with exposure time of 30 ms and 2-Hz sampling frequency. The temperature of the imaging chamber was maintained constantly at 37 °C throughout the experiment. Mean square displacement (MSD) and diffusion constant are calculated as previously described.[5d]

Supporting Information

Supporting Information is available from the Wiley Online Library or from the author.

Acknowledgements

S.J. and A.L. contributed equally to this work. We are grateful for the support from an AcRF tier 2 grant (T206B3220) to P.C.

Received: March 2, 2011
Revised: April 11, 2011
Published online: May 24, 2011

[1] B. S. Khakh, *Nat. Rev. Neuroscience* **2001**, *2*, 165.
[2] a) S. Hussl, S. Boehm, *Pfluegers Arch.* **2006**, *452*, 538; b) A. Surprenant, R. A. North, *Annu. Rev. Physiol.* **2009**, *71*, 333.
[3] B. S. Khakh, G. Burnstock, *Sci. Am.* **2009**, *301*, 84.
[4] a) G. H. Li, E. M. Lee, D. Blair, C. Holding, P. Poronnik, D. I. Cook, J. A. Barden, M. R. Bennett, *J. Biol. Chem.* **2000**, *275*, 29107; b) B. S. Khakh, W. B. Smith, C. S. Chiu, D. H. Ju, N. Davidson, H. A. Lester, *Proc. Nat. Acad. Sci. USA.* **2001**, *98*, 5288.
[5] a) M. Dahan, S. Lévi, C. Luccardini, P. Rostaing, B. Riveau, A. Triller, *Science* **2003**, *302*, 442; b) X. Michalet, F. F. Pinaud, L. A. Bentolila, J. M. Tsay, S. Doose, J. J. Li, G. Sundaresan, A. M. Wu, S. S. Gambhir, S. Weiss, *Science* **2005**, *307*, 538; c) A. M. Smith, H. W. Duan, A. M. Mohs, S. M. Nie, *Adv. Drug Delivery Rev.* **2008**, *60*, 1226; d) S. Lévi, C. Schweizer, H. Bannai, O. Pascual, C. Charrier, A. Triller, *Neuron* **2008**, *59*, 261; e) F. Pinaud, X. Michalet, G. Iyer, E. Margeat, H. P. Moore, S. Weiss, *Traffic* **2009**, *10*, 691; f) F. Pinaud, S. Clarke, A. Sittner, M. Dahan, *Nat. Meth.* **2010**, *7*, 275.
[6] H. W. Duan, M. Kuang, Y. A. Wang, *Chem. Mater.* **2010**, *22*, 4372.
[7] A. Matsumoto, S. Ikeda, A. Harada, K. Kataoka, *Biomacromolecules* **2003**, *4*, 1410.
[8] A. P. Liu, S. Peng, J. C. Soo, M. Kuang, P. Chen, H. W. Duan, *Anal. Chem.* **2011**, *83*, 1124.
[9] a) E. M. Hur, T. J. Park, K. T. Kim, *Am. J. Physiol.-Cell Physiol.* **2001**, *280*, C1121; b) G. Arslan, C. M. Catalin, E. Irenius, B. Kull, E. Clementi, C. Allgaier, D. Erlinge, B. B. Fredholm, *Neuropharmacology* **2000**, *39*, 482.
[10] A. Nicke, H. G. Baumert, J. Rettinger, A. Eichele, G. Lambrecht, E. Mutschler, G. Schmalzing, *EMBO J.* **1998**, *17*, 3016.
[11] F. Vacca, M. Giustizieri, M. T. Ciotti, N. B. Mercuri, C. Volonte, *J. Neurochem.* **2009**, *109*, 1031.
[12] a) J. Zhang, R. H. Xue, W. Y. Ong, P. Chen, *Biophys. J.* **2009**, *97*, 1371; b) F. Ye, A. Than, Y. Y. Zhao, K. H. Goh, P. Chen, *J. Endocrinol.* **2010**, *206*, 27.
[13] E. M. Zhang, R. H. Xue, J. Soo, P. Chen, *Pfluegers Arch.* **2008**, *457*, 211.
[14] J. C. Soo, J. Zhang, Q. Y. He, S. Agarwal, H. Li, H. Zhang, P. Chen, *Integr. Biol.* **2010**, *2*, 250.
[15] a) R. W. Holz, D. Axelrod, *Acta Physiol.* **2008**, *192*, 303; b) R. H. Xue, Y. Y. Zhao, L. Y. Su, F. Ye, P. Chen, *Pfluegers Arch.* **2009**, *458*, 1137.
[16] a) R. D. Murrell-Lagnado, O. S. Qureshi, *Mol. Membr. Biol.* **2008**, *25*, 321; b) S. J. Ennion, R. J. Evans, *Febs Letters.* **2001**, *489*, 154; c) O. S. Qureshi, A. Paramasivam, J. C. H. Yu, R. D. Murrell-Lagnado, *J. Cell Sci.* **2007**, *120*, 3838.
[17] a) N. Fujita, M. Kakimi, Y. Ikeda, T. Hiramoto, K. Suzuki, *Life Sci.* **2000**, *66*, 1849; b) D. B. Arthur, S. Georgi, K. Akassoglou, P. A. Insel, *J. of Neurosci.* **2006**, *26*, 3798.
[18] a) D. B. Arthur, K. Akassoglou, P. A. Insel, *Proc. Nat. Acad. Sci. USA.* **2005**, *102*, 19138; b) N. D'Ambrosi, B. Murra, F. Cavaliere, S. Amadio, G. Bernardi, G. Burnstock, C. Volonte, *Neurosci.* **2001**, *108*, 527.